Near Diffusion-Controlled Reaction of a $Zn(Cys)_4$ Zinc Finger with Hypochlorous Acid

Vincent Lebrun,[a,b,c] Jean-Luc Ravanat,[d,e] Jean-Marc Latour*[a,b,c] and Olivier Sénèque*[a,b,c]

[a] *Univ. Grenoble Alpes, LCBM/PMB, F-38000 Grenoble, France.*
[b] *CNRS, LCBM/PMB, UMR 5249, F-38000 Grenoble, France.*
[c] *CEA, BIG-CBM, PMB, F-38000 Grenoble, France.*
[d] *Univ. Grenoble Alpes, INAC-SCIB, F-38000 Grenoble, France.*
[e] *CEA, INAC-SyMMES, F-38000 Grenoble, France.*

E-mail: olivier.seneque@cea.fr ; jean-marc.latour@cea.fr

Electronic Supporting Information

Content

Materials and methods

N-α-Fmoc-protected amino acids for peptide synthesis, PyBOP coupling reagent and resins were obtained from Novabiochem or Iris Biotech. Other reagents for peptide synthesis, solvents, buffers and metal salts were purchased from Sigma-Aldrich. Analytical HPLC separations were performed on an Agilent Infinity 1200 system using PurospherStar (Merck) RP-18e 150 mm × 4.6 mm or Chromolith (Merck) RP-18e 100 mm × 4.6 mm columns at 1 and 2 mL/min, respectively. Preparative HPLC separations were performed on a VWR LaPrepΣ system using a XBridge Prep (Waters) C18 5 µm 150-19mm column. Mobile phase consisted in a gradient of solvent A (0.1% TFA in H_2O) and B (0.1% TFA in MeCN/H_2O 9:1) or C (0.1% TFA in MeOH/H_2O 9:1). ESI-MS analyses were performed on a Thermo LXQ spectrometer. LC/MS analyses were performed in Q1 MS mode using a Thermo Quantum Ultra electrospray mass spectrometer equipped with a Accela HPLC system. Separations were performed using an Uptisphere (Interchim) C18 10 x 2.1 mm, 3µm, column, eluted with a linear gradient of acetonitrile, from 0 to 30% in 30 min in 0.1% TFA, the flow rate being 200 µl/min. UV-Vis spectra were recorded on a Perkin-Elmer Lambda 35 spectrophotometer or on a Varian Cary 50 spectrophotometer. Fluorescence spectra were recorded on a Cary Eclipse spectrometer. Stopped-flow kinetic measurements were performed using a Bio-Logic SFM-400 stopped-flow device coupled to a MOS-450 AF-CD spectrometer equipped with a TC100/10F quartz cuvette (1 cm pathlength). The stopped-flow apparatus was thermo-regulated using circulating water bath. All buffer or metal solutions for spectroscopic measurements were prepared with MilliQ water (Millipore). Buffer solutions were treated with Chelex 100 resin (Biorad) to remove metal traces. HOCl solutions were prepared by dilution of a 2% NaOCl stock solution and stored at 4°C. The HOCl concentration was determined prior to use by measuring the absorbance at 292 nm (ε_{NaOCl} = 350 M^{-1} cm^{-1}) at pH 12.[1] Peptide L_{HSP} was synthesized as described previously.[2] Solutions of $Zn{\cdot}L_{HSP}$ were prepared under inert atmosphere (argon) by adding 1.1 eq. Zn^{2+} to a solution of free peptide (1-1.5 mM) in H_2O (exact concentration determined by Ellman's assay)[3] and adjusting the pH to 7.0 with NaOH and HCl.

Oxidation of $Zn{\cdot}L_{HSP}$ by HOCl: absorption and fluorescence titrations

A solution of $Zn{\cdot}L_{HSP}$ (20-40 µM) in a phosphate buffer (20 mM, pH 7.0 or 7.4) was prepared in a quartz cuvette by diluting the stock solution of complex into the buffer and water. For competition experiments, a solution of methionine in water was added to the cuvette. The titration was performed under air by addition of aliquots of a HOCl solution. Samples were equilibrated at 298 K after each HOCl addition, then absorption and fluorescence emission spectra were recorded. Absorption spectra were recorded every 1 nm at a scan rate of 240 nm min^{-1}. Fluorescence emission spectra were recorded with excitation at 280 nm every 1 nm.

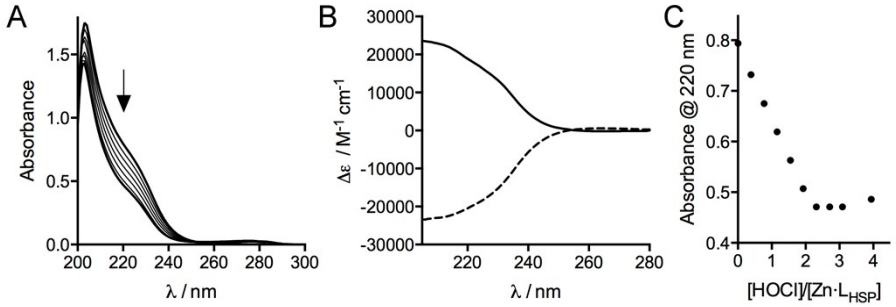

Figure S1. UV absorption monitoring of the titration of $Zn{\cdot}L_{HSP}$ (40 µM) in a phosphate buffer (20 mM, pH 7.0) by a HOCl solution (1 mM in water). (A) Evolution of the spectra upon HOCl addition (pathlength = 0.4 cm). (B) Difference spectrum obtained by subtracting the spectrum recorded after addition of 2.5 eq. HOCl to that of $Zn{\cdot}L_{HSP}$ (dashed line). The difference spectrum ($Zn{\cdot}L_{HSP} - L_{HSP}$), which corresponds to the LMCT absorption is shown as a solid line for comparison. Clearly, the change observed in the UV absorption spectrum during the titration can be ascribed to the loss of the LMCT absorption. (C) Plot of the absorbance at 220 nm against the number of equivalents of added HOCl *vs* $Zn{\cdot}L_{HSP}$.

Oxidation of Zn·L_{HSP} by HOCl: HPLC analyses

A solution of Zn·L_{HSP} (35 µM) in a phosphate buffer (50 mM, pH 7.0) was prepared by diluting a stock solution of Zn·L_{HSP} (*ca.* 400 µM) in the buffer and water (final volume 500 µL). An aliquot of a 20 mM HOCl solution (corresponding to 1-5 equivalent) was added to the complex solution. The mixture was stirred for 10 seconds and a methionine solution (100 mM, 50 µL) was added to destroy excess HOCl. After 30 s, the solution was analysed by analytical HPLC (Purospher Star RP-18e, 5 to 34% B gradient in 18 minutes, 1 mL/min).

Identification of bis-disulfide products

The three bis-disulfide forms of L_{HSP} were prepared by reacting Zn·L_{HSP} in a phosphate buffer (100 mM, pH 7.0) with H_2O_2 or HOCl on a preparative scale (10 mg Zn·L_{HSP} in 3 mL buffer). Bis-disulfides were separated by preparative HPLC and lyophilized. Oxidized peptides (0.25 mg) were dissolved in a phosphate (25 mM, pH 7.0, 250 µL). Trypsin (100 µg/mL, 30 µL) or both Trypsin (100 µg/mL, 30 µL) and/or Glutamate carboxypeptidase GluC (200 ng/mL, 20 µL) were added. Solutions were incubated overnight at 37°C and analysed by LC/MS. Trypsin hydrolyses peptide bond at carboxylic side of lysine and arginine. GluC hydrolyses peptide bond at carboxylic side of glutamate and aspartate. Possible hydrolysis sites are shown on Figure S2.

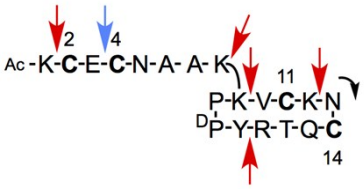

Figure S2. Hydrolysis sites for trypsin (red) and GluC (blue) in L_{HSP}.

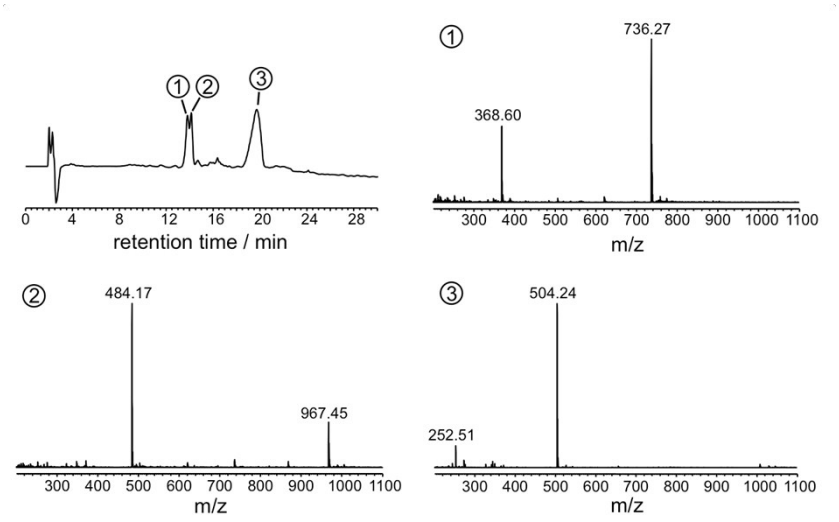

Figure S3. LC/MS analysis of Trypsin and GluC digestion of L_{HSP} bis-disulphide isomer α.

Stopped-flow experiments

The kinetics of the reaction of Zn·L_{HSP} with HOCl (or ClO^-) was measured on a Biologic stopped-flow apparatus with the following typical procedure at various pH values. For this purpose, a set of phosphate buffer solutions (20 mM, ionic strength I = 0.62 ± 0.02) covering the pH range 10.5-13.5 was prepared by diluting stock solutions of Na_2HPO_4 0.1 M and $NaClO_4$ 0.8 M and adjusting the pH to the desired value using NaOH. Stock solutions of Zn·L_{HSP} (1-1.5 mM) and NaOCl (2-5 mM) were prepared in water (their concentration was determined as described above). Prior to stopped-flow experiments, these stock solutions were diluted with a

phosphate buffer to 2-10 µM and 50-800 µM, respectively. The four syringes of the stopped-flow apparatus were filled with water, buffer, NaOCl solution and $Zn{\cdot}L_{HSP}$ solution and the temperature was maintained at 25°C using a circulating bath. Lines were thoroughly washed with water and buffer before each shot, which consisted of the fast mixing of buffer, NaOCl and $Zn{\cdot}L_{HSP}$ solutions in various proportions. The reaction was monitored by recording the decay of the $RS^- \rightarrow Zn^{2+}$ ligand to metal charge transfer absorption at 230 nm (this wavelength was a compromise between the intensity of the absorption band and the light intensity of the lamp). The recording time was adjusted from 160 ms to 8 ms in order to record the full kinetics and ensure that a plateau is reached. The NaOCl and $Zn{\cdot}L_{HSP}$ concentrations were varied by changing the volume ratio of the mixed solutions but always keeping $[NaOCl] > 10\times[Zn{\cdot}L_{HSP}]$ so as to maintain pseudo-first-order conditions. For each condition, shots were accumulated, aberrant data were removed and kinetic traces were averaged to reduce noise. The pseudo-first-order rate constant k^{obs} (s^{-1}) was determined by fitting the averaged trace to a mono-exponential decay. In order to check that the absorbance decay corresponds to the oxidation of the four cysteines, the amplitude of the absorbance decay at 230 nm (pH 12) was compared to the absorbance loss at 230 nm obtained by steady-state absorption measurements during the titration of $Zn{\cdot}L_{HSP}$ by HOCl at pH 12. The amplitude of the kinetic traces corresponded to $\Delta\varepsilon$ = 10 500 ± 1 500 M^{-1} cm^{-1}, which is in good agreement with the value of 12 000 M^{-1} cm^{-1} obtained by steady-state measurements (Figure S4A) and thus oxidation of the four cysteines during the observed reaction. The order of the reaction relative to NaOCl was obtained by a plot of $\log(k^{obs})$ against $\log([NaOCl]_0)$ where $[NaOCl]_0$ is the initial concentration of added hypochlorite. For instance, at pH 12.6, a slope of 0.99 ± 0.05 was obtained by linear regression, in agreement with a first-order reaction relative to NaOCl (Figure S4B). Apparent second-order rate constant k_{app} (M^{-1} s^{-1}) at each pH value was determined by linear regression of the [NaOCl]-dependence of k^{obs}.

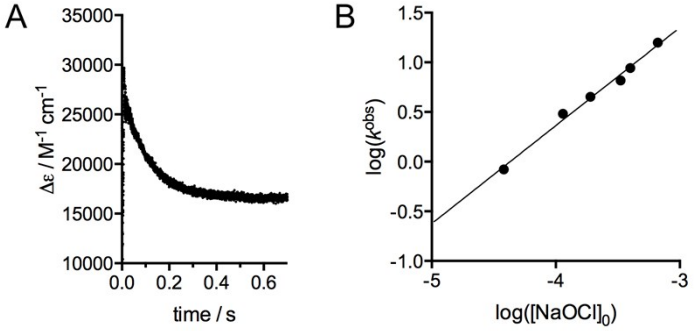

Figure S4. (A) Example of kinetic trace measured at pH 12.0 with $[Zn{\cdot}L_{HSP}]$ = 1.0 µM and $[NaOCl]_0$ = 167 µM. (B) Determination of reaction order relative to NaOCl: plot of $\log(k^{obs})$ against $\log([NaOCl]_0)$ at pH 12.6. Linear regression gives a slope of 0.99 ± 0.05.

Oxidation of methionine by HOCl: re-evaluation of the rate constants

Competition experiments between FmocMet and Met were performed in order to determine the second-order rate constant of Met oxidation. For this purpose, solutions containing FmocMet ($[FmocMet]_0$ = 20 µM) and Met ($[Met]_0$ = 10-40 µM) or FmocMet only (20 µM) were prepared in a phosphate buffer (10 mM) at pH 7.4 and oxidized with the same amount of HOCl (2.5-10 µM). The fluorescence spectra were recorded before and after addition of HOCl. Then, excess HOCl was added for complete oxidation of FmocMet and the fluorescence spectrum was recorded again. For each solution, the yield of FmocMetO can be calculated form such a set of three spectra. The concentration-dependent inhibition of FmocMetO formation by Met was analysed using the standard competition kinetic approach described by Storkey *et al*. with Equations 1 and 2, where Y_{max} and Y_{Met} are the yields of FmocMetO formation in the absence and presence of Met, respectively.[4] Figure S5 shows the data obtained for these competitions, which give $k_{app}(Met)/k_{app}(FmocMet)$ = 1.22 ± 0.03.

$$\frac{Y_{Met}}{Y_{max} - Y_{Met}} = \frac{k_{app}(FmocMet)}{k_{app}(Met)} \times \frac{[FmocMet]_0}{[Met]_0} \quad (1)$$

$$\frac{Y_{max}}{Y_{Met}} \times [FmocMet]_0 = \frac{k_{app}(Met)}{k_{app}(FmocMet)} \times [Met]_0 + [FmocMet]_0 \quad (2)$$

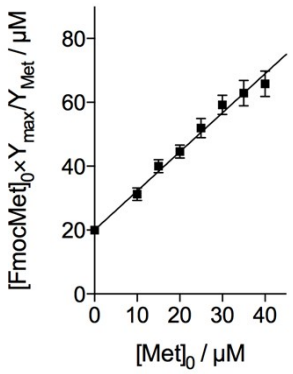

Figure S5. Competitive oxidation of FmocMet and Met by HOCl at pH 7.4 monitored by fluorescence in a phosphate buffer (10 mM, 298 K): plot of $[FmocMet]_0 \times Y_{max}/Y_{Met}$ against $[Met]_0$. The slope gives $k_{app}(Met)/k_{app}(FmocMet) = 1.22 \pm 0.03$.

Alternative kinetic analysis of each competition experiment with Equation 3, where $[FmocMet]_f$ and $[Met]_f$ are the concentrations of FmocMet and Met after oxidation by HOCl, was also performed as proposed by Storkey *et al.*[4] This gave the same ratio within error margin: $k_{app}(Met)/k_{app}(FmocMet) = 1.29 \pm 0.12$. Therefore, our competition experiments lead to a new experimental value for $k_{app}(Met)$ at pH 7.4, $(1.9 \pm 0.3) \times 10^8$ M^{-1} s^{-1}, which is *ca.* one order of magnitude higher than that proposed by Storkey *et al.*

$$\frac{k_{app}(Met)}{k_{app}(FmocMet)} = \frac{\ln\left(\frac{[Met]_0}{[Met]_f}\right)}{\ln\left(\frac{[FmocMet]_0}{[FmocMet]_f}\right)} \quad (3)$$

Simulation of competitive oxidation of $Zn{\cdot}L_{HSP}$ and methionine by HOCl

The fluorescence titrations of $Zn{\cdot}L_{HSP}$ in the presence of methionine at pH 7.0 and 7.4 were simulated using the program SPECFIT. For this purpose, we used the following kinetic model (Equations 4-6), where A is the oxidant, regardless of its protonation state, B is $Zn{\cdot}L_{HSP}$, C and D are the mono-disulfide and bis-disulfide forms of L_{HSP}, respectively, E is methionine and F is methionine sulfoxide. For simulations, k_3 was kept constant and equal to the apparent second-order rate constant of the reaction between methionine and HOCl, $k_{app}(Met)$, determined for pH 7.0 or 7.4, the ratio k_1/k_3 was varied and the ratio k_2/k_1 was kept constant and equal to 10. The final concentration of $Zn{\cdot}L_{HSP}$ was calculated for various values of the HOCl concentration. The change in fluorescence emission was assumed to be proportional to the change of concentration of $Zn{\cdot}L_{HSP}$ (Note: several values were tested for the ratio k_2/k_1, from 5 to 20, but this had a negligible influence on the final $Zn{\cdot}L_{HSP}$ concentration and on the shape of the simulated fluorescence decay). Figure S6 shows an example of simulations with $[Zn{\cdot}L_{HSP}] = 20$ µM and [Met] = 190 µM at pH 7.4. Best agreement between experimental data at pH 7.4 and simulations was obtained with $k_1/k_3 = 1.75$ at both pH values.

$$A + B \xrightarrow{k_1} C \quad (4)$$

$$A + C \xrightarrow{k_2} D \quad (5)$$

$$A + E \xrightarrow{k_3} F \quad (6)$$

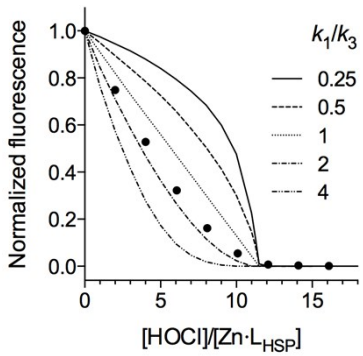

Figure S6. Simulation of tyrosine fluorescence change in competitive oxidation of $Zn{\cdot}L_{HSP}$ (20 µM) and methionine (190 µM) by HOCl at pH 7.4. Simulations were performed with $k_3 = 3.2\times10^8$ M^{-1} s^{-1}, $k_2 = 10\times k_1$ and $k_1/k_3 = 0.25$, 0.5, 1, 2 and 4. Black circles correspond to the experimental titration.

References

[1] J. C. Morris, *J. Phys. Chem.* **1966**, *70*, 3798–3805.

[2] O. Sénèque, E. Bourlès, V. Lebrun, E. Bonnet, P. Dumy, J.-M. Latour, *Angew. Chem., Int. Ed.* **2008**, *47*, 6888–6891.

[3] P. W. Riddles, R. L. Blakeley, B. Zerner, *Methods Enzymol.* **1983**, *91*, 49–60.

[4] C. Storkey, M. J. Davies, D. I. Pattison, *Free Radic. Biol. Med.* **2014**, *73*, 60–66.